



***PRC1* promotes cell proliferation and cell cycle progression by regulating *p21/p27-pRB* family molecules and *FAK-paxillin* pathway in non-small cell lung cancer**

Zhigang Liang, Xinjian Li, Jian Chen, Haina Cai, Liqun Zhang, Chenwei Li, Jingjie Tong, Wentao Hu

Department of Thoracic Surgery, Ningbo First Hospital, Ningbo 315000, China

Contributions: (I) Conception and design: Z Liang; (II) Administrative support: Z Liang; (III) Provision of study materials or patients: Z Liang, X Li, J Chen; (IV) Collection and assembly of data: H Cai, L Zhang, C Li; (V) Data analysis and interpretation: Z Liang, J Tong, W Hu; (VI) Manuscript writing: All authors; (VII) Final approval of manuscript: All authors.

Correspondence to: Zhigang Liang, Department of Thoracic Surgery, Ningbo First Hospital, No. 59, Liuting Street, Ningbo 315000, China. Email: 39908517@qq.com.

Background: This study aimed to demonstrate the function and molecular mechanism of protein regulator of cytokinesis 1 (*PRC1*) in the carcinogenesis of non-small cell lung cancer (NSCLC).

Methods: Bioinformatics analysis was performed. Cell culture and plasmid construction were conducted for cell transfection. mRNA and protein expression, cell proliferation, migration, and cell cycle were detected. Mice models were also constructed. The relationship between *PRC1* and the prognosis of NSCLC patients was analyzed.

Results: *PRC1* expression was higher in tumor tissues than adjacent non-tumor tissues ($P<0.05$). Cells transfected with the high-expression *PRC1* plasmid (TOPO-*PRC1* group) had the stronger ability of proliferation and migration ($P<0.05$) along with a lower incidence of stay at the G2/M phase ($P<0.05$) than the low-expression *PRC1* plasmid. Mice models showed tumors obtained from mice in the TOPO-*PRC1* group significantly grew faster, larger, and heavier ($P<0.05$) than the low-expression *PRC1* group. Among the 150 NSCLC patients, patients with the higher *PRC1* expression were more likely to have lymph node metastasis occur ($P<0.05$) and progress into an advanced stage ($P<0.05$), and showed shorter survival ($P<0.05$). Moreover, the TOPO-*PRC1* group had a lower phosphorylation level, and a lower expression of *Cip1/p21* ($P<0.05$) and *Kip1/p27* ($P<0.01$).

Conclusions: *PRC1* could promote cell proliferation and cell cycle progression through *FAK-paxillin* pathway molecules and the regulation of the phosphorylation level of *p21/p27-pRB* family molecules. *PRC1* might be a new and promising therapeutic target for NSCLC.

Keywords: Protein regulator of cytokinesis 1 (*PRC1*); non-small cell lung cancer (NSCLC); cell proliferation; cell cycle; prognosis

Submitted Aug 20, 2019. Accepted for publication Sep 11, 2019.

doi: 10.21037/tcr.2019.09.19

View this article at: <http://dx.doi.org/10.21037/tcr.2019.09.19>

Introduction

Lung cancer is the leading causes of cancer death around the world, with projected 154,050 lung cancer deaths occurring in 2018, and an estimated 234,030 new cases of lung cancer being diagnosed (1). Although various strategies have been applied to improve the treatment

regimen for lung cancer, the 5-year survival of lung cancer is 10–20% in most countries (2,3). At present, there is still a lack of understanding of the molecular mechanism in the carcinogenesis of non-small cell lung cancer (NSCLC), which is the most common subtype of lung cancer (4).

Evidence shows that precise diagnosis and therapy are

beneficial for improving survival of patients with lung cancer (5). Thus, it is essential to identify the carcinogenesis of lung cancer and therefore to find promising therapeutic targets. Through gene expression profile chip data analysis, the establishment of molecular marker groups related to the occurrence and development of lung cancer can provide abundant information for treatment (6). Mutations of *EGFR*, *KRAS*, and *ALK* have been demonstrated to be associated with the carcinogenesis of lung cancer (7). Consequently, various first-line drugs have been manufactured to realize precise target therapy (8).

Via analyzing three groups of gene expression profile data of NSCLC patients (GSE42127, GSE11969, GSE8894) from the Gene Expression Omnibus (GEO) database (9), a group of differential genes related to the malignant phenotype and poor prognosis of NSCLC were found, including *AURKA*, *PRC1*, *COL17A1*, and *CDKN3*. A protein regulator of cytokinesis 1 (PRC1), belonging to the microtubule-associated proteins (MAPs) family, is located on chromosome 15 in humans (10). *PRC1* was originally identified as a mitotic spindle-associated cyclin-dependent kinase (Cdk) substrate *in vitro*, which encodes a protein present at high levels during the S and G2/M phases of mitosis (11). *PRC1* has been subsequently regarded as a microtubule binding and bundling protein that maintains the midzone of the mitotic spindle (12). Microtubules play essential roles in the cell cycle, along with cell trafficking, signaling transduction, and cell migration (13). Alterations in microtubule-associated proteins have been demonstrated in carcinogenesis (14).

Growing evidence indicates that *PRC1* is overexpressed in some malignant tumors and plays an important role in tumor progression (15,16). However, the function and molecular mechanism of *PRC1* in the carcinogenesis of NSCLC are still unclear. This study aimed to identify the function and molecular mechanism of *PRC1* in NSCLC, and further provide therapeutic targets for NSCLC patients in clinical practice.

Methods

Bioinformatics analysis

Gene expression profile and clinical outcomes of 285 patients with stage I–III were obtained from three datasets of GEO (GSE42127, GSE11969, GSE8894) (Table S1). All data were screened based on flag filtering, fold change filtering, and expression level filtering, and then

selected data were standardized by the LOWESS method. Differentially expressed genes (DEGs) were selected and presented by Student's *t*-test, similar sample research, scatter plot, cluster/gene tree, and Venn diagram. The KEGG pathways of 35 differentially expressed key genes were analyzed online by DAVID. The DEG sets were analyzed based on the database of KEGG biological pathways (<http://www.genome.jp/>). Meanwhile, gene ontology (GO) annotation and functional cluster analysis were applied to screen DEGs which were related to the poor prognosis of lung cancer. TELiS online and GATHER online were used to predict binding sites of transcription factors in DEGs. STRING online analysis was used to predict the expression patterns of DEGs. Moreover, the key DEGs were verified by analyzing their expression levels in tissues from TCGA datasets, and performing quantitative real-time polymerase chain reaction (q-PCR) based on 36 tumor tissues and corresponding adjacent non-tumor tissues collected from our institution.

Cell culture

NSCLC cell lines A549 and NCL-H358 were purchased from Institutes for Biological Science, Chinese Academy of Science. A549 and NCL-H358 cells were cultured in RPMI-1640 containing 10% fetal bovine serum at 37 °C in a humidified incubator containing 5% CO₂.

Clinical sample collection

Patients who met the following criteria were enrolled in our study: (I) pathologically diagnosed with NSCLC from 2015 to 2016 in Ningbo First Hospital; (II) no chemotherapy or radiation received before surgery. Tumor tissues and corresponding adjacent non-tumor tissues at a minimum distance of 5 cm from tumor tissue were collected. Clinical data were also obtained from medical records. This study was approved by the Ethics Committee of Ningbo First Hospital, and informed consent was signed by all participants.

RNA extraction and q-PCR

TRIzol reagent (Invitrogen, Carlsbad, CA, USA) was used to extract total RNA of cultured cells and tissue samples. Total RNA concentrations, purity, and integrity were also assessed. Reverse transcription was carried out to obtain cDNA by Primer Script RT-reagent Kit (TaKaRa), while

q-PCR was performed by SYBR Green PCR master mix. GAPDH was considered as an internal reference for relative quantitative analysis (Table S2).

Western blot (WB)

After being transfected with highly expressed PRC1 plasmid or siRNA-PRC1, cultured cells were lysed by lysis buffer (RIPA, KeyGEN) with protease inhibitors (PMSF, KeyGEN) on ice for 30 minutes. A BCA Kit (KeyGEN) was used to determine protein concentration. Approximately 30 µg of lysate protein was used for WB. Polyvinylidene fluoride (PVDF) was scanned by ChemiDoc™ XRS (Bio-Rad), and β-actin or GAPDH was regarded as the candidate protein.

Plasmid construction and cell transfection

The plasmids with high *PRC1* expression and an empty vector were provided by GenePharma, Shanghai, China. The plasmids with a high expression of *PRC1*, empty vector, siRNA-PRC1, and siRNA- negative control (NC) were each transfected into NSCLC cells via Opti-MEM mediums containing Lipofectamine 3000 (Invitrogen, Carlsbad, CA, USA) and plasmid NDA. The transfection efficiency was assessed 48 hours after transfection. Q-PCR and WB were performed to determine the expression of *PRC1* mRNA and *PRC1* protein, respectively (Table S3).

Soft agar assay

The 0.3% upper soft agar was configured with low melting agarose and 2×RPMI-1640 mediums (Corning, NY, USA). After adding 0.3% upper soft agar into 6-well plates containing 0.6% underlying soft agar, 100 µL single cell suspensions were seeded. After a 2–3 weeks culture, inverted fluorescence microscope, combined with the following formula, was used to evaluate cell proliferation: proliferation efficiency (PE) = (colony number/inoculated cell number)*100%.

Cell transwell

RPMI-1640 medium with 500 µL of 10% fetal bovine serum, 100 µL serum-free RPMI-1640, and 3×10^4 cells were added into the lower chamber of a transwell (Corning, NY, USA) for 12 hours at 37 °C. After culture, the cells on the upper surface of the membrane were wiped off, while the

cells on the lower surface of the membrane were fixed with paraformaldehyde for 15 minutes and stained with crystal violet for 5 minutes. The cells fixed on the lower surface of the membrane were counted by microscope.

Flow cytometry

Negative control and NSCLC cells after transfection were digested and blown into cell suspension. After repeated PBS washing and centrifugation, RnaseA and PI were added to the PBS containing cells. Then, 500 µL of this mixture were stained in a cell incubator at 37 °C, and Beckman Coulter Fc500 was applied to analyze the distribution of cell cycle.

Immunohistochemistry

To deparaffinize and rehydrate tissue sections, 95%, 90%, 85%, 80%, and 70% alcohol were used, while 3% H₂O₂ was applied to block endogenous peroxidase activity. Antigen retrieval was performed by 5% sheep serum. After adding PRC1 antibodies (Abcam), diaminobenzidine (DAB) was used for immunostaining. A microscope was used to evaluate staining intensity and the percentage of positive staining cells, while Olympus imaging system was applied to quantitatively analyze the staining results of PRC1 protein. The mean optical density (MOD) was used to assess the expression level of PRC1.

Animal experiments

All animal experiments were performed based on the NIH animal use guidelines and approved by the Ethics Committee of Ningbo First Hospital. The plasmids with a high-expression of PRC1 and empty vector were each transfected into tumor cells. Then, 10 mice (Laboratory Animal Resources, Chinese Academy of Science) were used for tumor transplantation, and 200 µL cell suspension was injected into each selected mouse aged 4–6 weeks and weighing 18–22 kg. The volume of tumor was calculated by the length and weight of the tumor. The growth curve of the tumor was also plotted. Tumor tissues were obtained about 5 weeks after transplantation.

Cell immunofluorescence assay

After being transfected for 72 hours, cells were digested and suspended. After fixation and washing by PBS, fluorescent antibodies (Santa Cruz Biotechnology) were added and

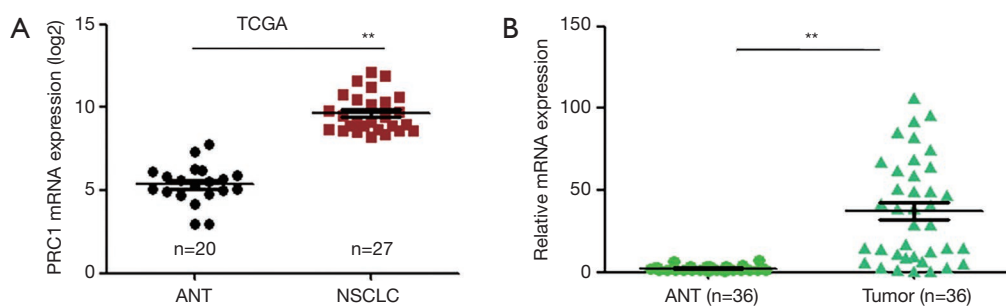


Figure 1 The expression of *PRC1* between adjacent non-tumor (ANT) tissue and non-small cell lung cancer (NSCLC). (A) The comparison of *PRC1* expression between ANT and NSCLC from TCGA database. (B) The comparison of *PRC1* expression between ANT tissues and tumor tissues from 36 NSCLC patients by q-PCR. PRC1, protein regulator of cytokinesis 1.

Table 1 The characteristics of 36 enrolled patients

Patient parameters (n=36)	Number
Sex (male/female)	20/16
Age (years old)	
>60	21
≤60	15
Smoking status (smoking/non-smoking)	19/17
Maximum diameter of primary tumor	
≤3 cm	23
>3 cm	13
Lymphatic metastasis (+/-)	12/24
TNM stage (I/II/III/IV)	13/15/8/0
Subtypes of lung cancer	
Squamous cell carcinoma	14
Adenocarcinoma	21
Large cell lung cancer	1

reacted with antigens. An inverted fluorescence microscope was used to assess the fluorescence signal of each group. Image J software was used to analyze immunofluorescence intensity (IOD).

Cell counting kit-8 (CCK-8)

All tumor cells were plated into 96-well plates and each well contained 100 μ L culture medium and 5×10^3 cells. All tumor cells after transfection were divided into 4 groups: the plasmids with a high-expression of PRC1, empty vector, PRC1-siRNA-negative control, and PRC1-siRNA-FAK.

Each well was infused with 10 μ L CCK-8 reagent (Dojindo, Japan) after transfection for 48 hours. Then, all tumor cells were incubated at 37 $^{\circ}$ C for 2 hours. When the color of the culture medium became orange, ELISA (Bio-Rad) was used to detect absorbance at 450 nm to evaluate the impact of PRC1 on the proliferation of NSCLC cells and the mechanisms regulated by the FAK pathway.

Statistical analysis

All continuous data are expressed as mean \pm standard. Student's *t*-test was conducted to analyze any differences between the two groups. Kaplan-Meier and log-rank tests were performed to analyze the relationship between the expression level of PRC1 and the survival of patients. $P < 0.05$ was marked as *, indicating statistical difference; while $P < 0.01$ was marked as **, indicating statistically significant difference.

Results

PRC1 may be a potential oncogene of NSCLC

Altogether, 35 DEGs including 29 upregulated genes were identified by GSE42127, GSE11969, and GSE8894. Most of the upregulated genes were associated with cell cycle, extracellular matrix receptor regulation, and cell movement. After reviewing other studies (17,18), PRC1, which might be related to the poor prognosis of NSCLC, was selected as our target. The TCGA dataset indicated that the expression level of *PRC1* in tumor tissue was higher than that of adjacent non-tumor tissues in NSCLC ($P < 0.01$) (Figure 1A). The characteristics of the 36 enrolled patients are shown in Table 1. Q-PCR reconfirmed that the higher expression of *PRC1* mRNA in tumor tissue in NSCLC ($P < 0.01$) (Figure 1B).

PRC1 overexpression promoted NSCLC cell proliferation and migration, and accelerated the process of cell cycle in vitro

Cells transfected with highly expressed PRC1 plasmids, empty vector, siRNA-PRC1, and siRNA-NC, were divided into the TOPO-PRC1 group, TOPO-Vector group, siRNA-PRC1 group, and siRNA-NC group, respectively. Compared with the TOPO-Vector group, PRC1 protein and mRNA expression of cells were upregulated significantly in the TOPO-PRC1 group ($P < 0.01$) (Figure 2A). Compared with the siRNA-NC group, cells in the siRNA-PRC1 group had down-regulated PRC1 protein and mRNA expression ($P < 0.01$) (Figure 2B). Soft agar assay showed that cells in TOPO-PRC1 group had significantly higher PE than those in the control group, while lower PE appeared in the siRNA-PRC1 group, compared with the TOPO-Vector group ($P < 0.05$) (Figure 2C,D).

PRC1 expression level was related to NSCLC cell cycle and its migration

Flow cytometry indicated that compared with TOPO-PRC1 group, TOPO-Vector group had more cells in the G2/M phase ($8\% \pm 0.53\%$ vs. $12\% \pm 0.75\%$) and less cells in the S phase, with the differences being significant ($P < 0.05$) (Figure 3A,B). Cell transwell showed that compared with the other 3 groups, more NSCLC cells in the TOPO-PRC1 group migrated to the lower surface of the membrane ($P < 0.05$) (Figure 3C,D).

The upregulation of PRC1 expression promoted tumor growth in mice

No mice died before the removal of tumor tissues, and tumors were obtained from all mice. Tumors in the mice of the TOPO-PRC1 group grew faster, and from the third week of transplantation, the difference of tumor size gradually became great ($P < 0.05$). The TOPO-PRC1 group had larger tumor sizes and significantly heavier tumor weight than the TOPO-Vector group (Figure 4).

The high expression of PRC1 was associated with late stage and poor prognosis for NSCLC patients

A total of 150 eligible NSCLC patients were included to assess the relationship between PRC1 expression and survival of NSCLC patients. For 150 included patients, the 1-year follow-up rate, 3-year follow-up rate, and 5-year

follow-up rate were 100%, 83.6%, and 61.2%, respectively. Only 1 patient was lost to follow-up after 3 years. The basic characteristics of the 150 patients are shown in Table 2. The immunohistochemical results not only indicated that PRC1 protein was mainly located in the cytoplasm and partially in the nucleus, but also suggested that patients with different stages had different staining intensity (Figure 5A). For stage III NSCLC patients, the tumor tissue had significantly higher MOD than that of patients with other stages, and the MOD of tumor tissue was higher than that of adjacent non-tumor tissue in stage III patients, but not for patients with other stages (Figure 5B). In addition, higher PRC1 expression was also related to lymph node metastasis and adenocarcinoma ($P < 0.05$). Survival analysis implied a significantly meaningful trend towards shorter overall survival and progression free survival with the higher PRC1 expression ($P < 0.05$) (Figure 5C).

PRC1 promoted NSCLC proliferation by regulating the phosphorylation of molecules in the FAK-Paxillin pathway

All experiments of CCK-8 showed that the NSCLC cells in the TOPO-PRC1 group had a higher ability of proliferation compared with that in the TOPO-Vector group (** $P < 0.01$). Meanwhile, the proliferation capacity of NSCLC cells in the PRC1+siRNA-FAK group was significantly lower than that in the PRC1+siRNA-NC group (** $P < 0.01$) (Figure 6).

WB was performed to detect the phosphorylation level of several major phosphorylation sites at the N-terminal, C-terminal, and the kinase activation ring of NSCLC cells in the 4 groups. In the TOPO-PRC1 group, the FAK pY397, FAK Py576/577, and FAK pY925 of NSCLC cells showed a significantly higher phosphorylation level than those cells in the TOPO-vector group, which was in line with the quantitative analysis of the Gel pro analyzer 4.0 (* $P < 0.05$) (Figure 7A). Moreover, the Gel pro analyzer 4.0 also showed that the difference in the phosphorylation level of FAK pY576/577 between the TOPO-PRC1 group and TOPO-Vector group was greatest (** $P < 0.01$) (Figure 7B). The expression of FAK pY397, FAK pY576/577, and FAK pY925 significantly decreased in the siRNA-PRC1 group (** $P < 0.01$) (Figure 7C).

WB also implied that the phosphorylation level of paxillin, the downstream target of FAK signaling pathway, was upregulated in the TOPO-PRC1 group (Figure 7D), while the phosphorylation level of paxillin was down-regulated in the siRNA-PRC1 group (* $P < 0.05$) when compared with that of the TOPO-Vector group and

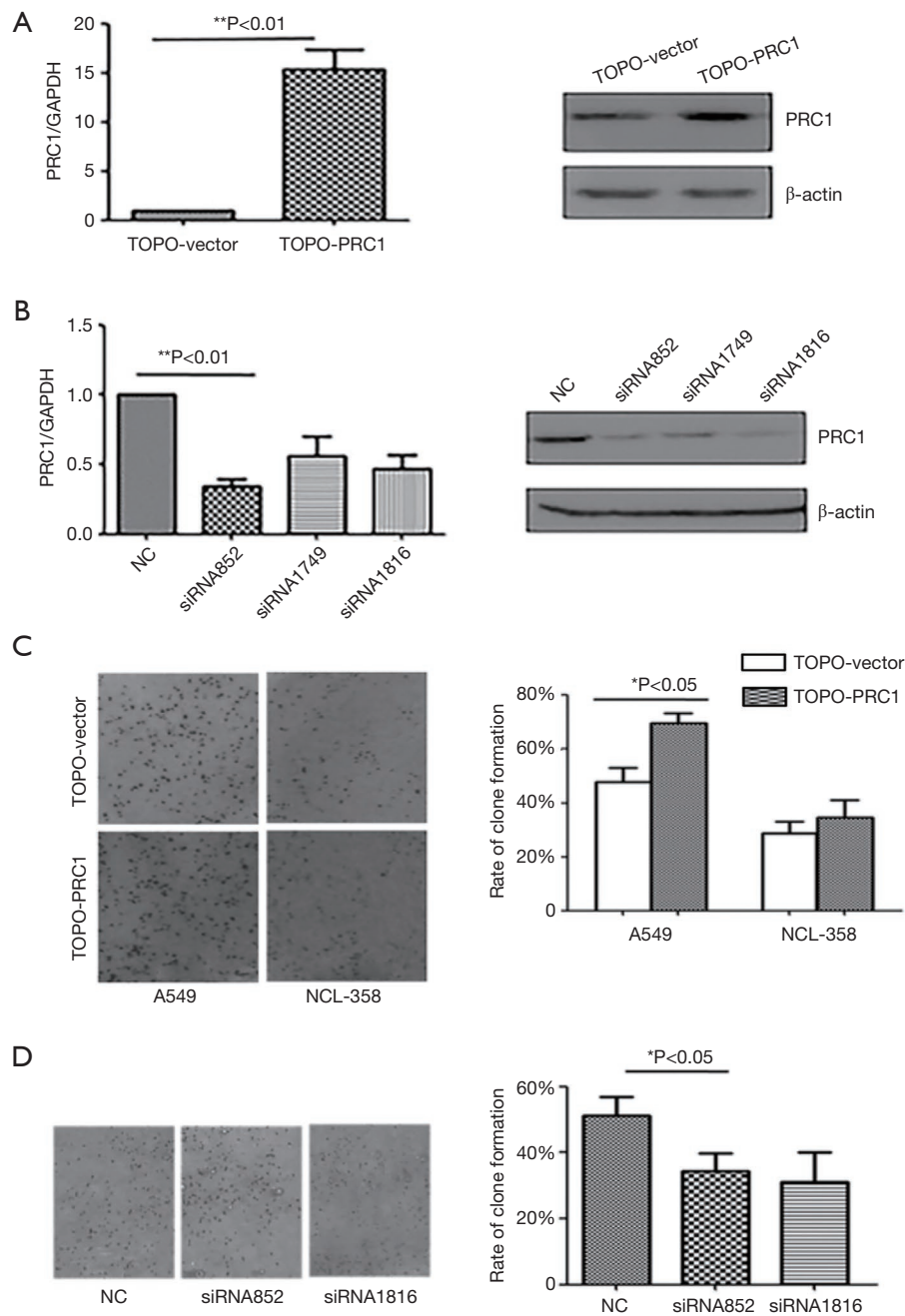


Figure 2 Comparison of PRC1 mRNA, PRC1 protein and cell proliferation capacity among different groups. Cells transfected with highly expressed PRC1 plasmids, empty vector, siRNA-PRC1, and siRNA-negative control were divided into the TOPO-PRC1 group, TOPO-Vector group, siRNA-PRC1 group, and siRNA-NC group, respectively. (A) The comparison of PRC1 mRNA and protein between the TOPO-PRC1 group and the TOPO-Vector group. (B) The comparison of PRC1 mRNA and protein between the siRNA-PRC1 group and the siRNA-NC group by q-PCR. (C) The comparison of cell proliferation capacity between TOPO-PRC1 group and TOPO-Vector group ($\times 100$). (D) The comparison of cell proliferation capacity between siRNA-PRC1 group and siRNA-NC group ($\times 100$). PRC1, protein regulator of cytokinesis 1.

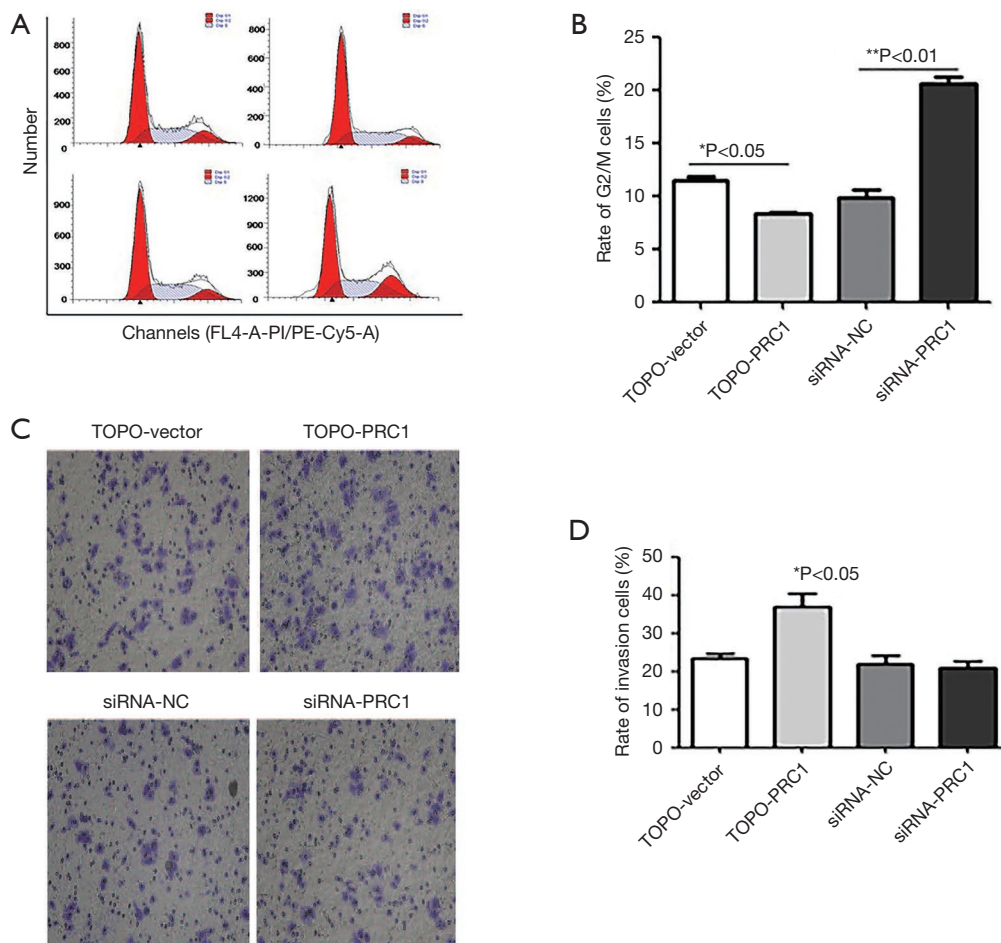


Figure 3 The cell cycle of cells in different groups. Cells transfected with highly expressed PRC1 plasmids, empty vector, siRNA-PRC1, and siRNA-negative control were divided into the TOPO-PRC1 group, TOPO-Vector group, siRNA-PRC1 group, and siRNA-NC group, respectively. (A) The cell cycle of NSCLC cells in different groups by flow cytometry. Ordinate: cell number, ordinate: DNA content. (B) Distribution ratio of NSCLC cells in the G2/M phase of different groups. (C) The results of cell transwell (stained by crystal violet, $\times 100$). (D) Quantitative analysis of Cell transwell. PRC1, protein regulator of cytokinesis 1; NSCLC, non-small cell lung cancer.

siRNA-NC group, respectively (Figure 7E,F).

PRC1 influenced the NSCLC cell cycle by regulating the phosphorylation of p21/p27 and pRB family molecules

Immunofluorescence showed that the TOPO-PRC1 group had a higher IOD of F-actin than that of the TOPO-Vector group (Figure 8A,B). Compared with those in the TOPO-Vector group, cells in the TOPO-PRC1 group had lower expression of Cip1/p21 mRNA ($*P < 0.05$) and Kip1/p27 mRNA ($**P < 0.01$). Meanwhile, WB indicated that the TOPO-PRC1 group also had higher expressions of both Cip1/p21 and Kip1/p27 protein (Figure 8C). Furthermore,

NSCLC cells in the TOPO-PRC1 group showed lower phosphorylation levels of p107 and p130 than those in the TOPO-Vector group, while no difference was found in the phosphorylation levels of pRB between these 2 groups (Figure 8D).

Discussion

Our trials showed a high expression of PRC1 could promote the proliferation and migration of NSCLC cells, and the growth of NSCLC xenografts in mice. These results strongly confirm that the upregulation of PRC1 expression may play an important role in the occurrence

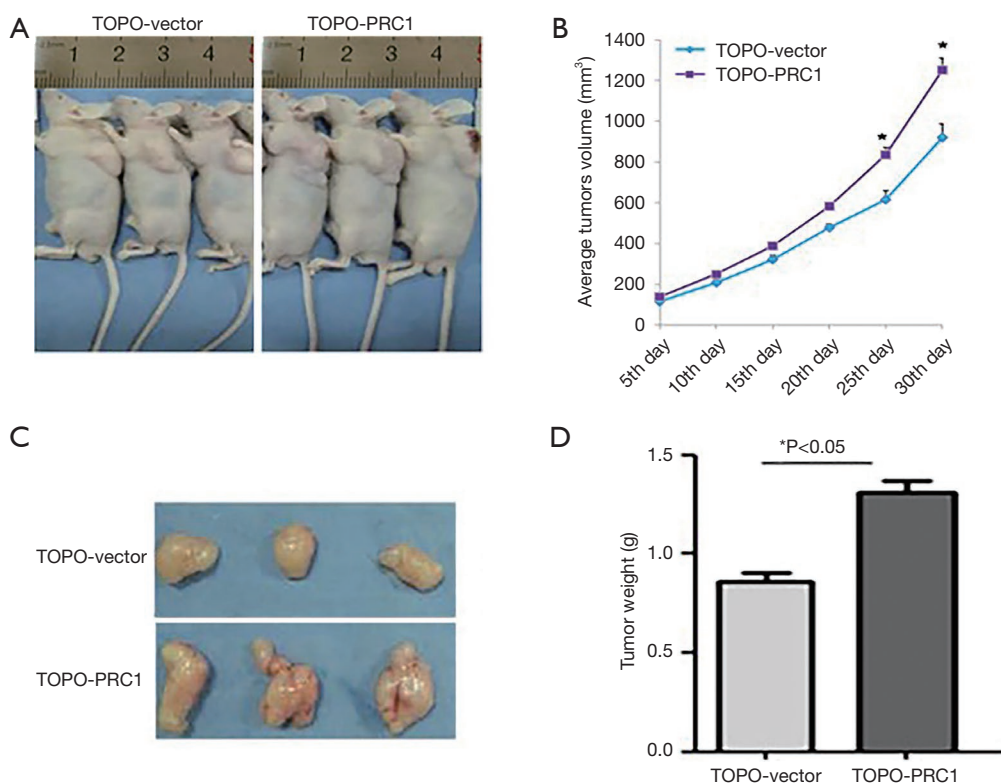


Figure 4 The results of animal experiments. Cells transfected with highly expressed PRC1 plasmids, empty vector, siRNA-PRC1, and siRNA-negative control were divided into the TOPO-PRC1 group, TOPO-Vector group, siRNA-PRC1 group, and siRNA-NC group, respectively. (A) The mice were transplanted with tumors. (B) The growth curve of transplanted tumor. (C) The comparison of transplanted tumor size and weight of mice between the TOPO-Vector and TOPO-PRC1 group. (D) The comparison of transplanted tumor weight of mice between the TOPO-Vector and TOPO-PRC1 group. PRC1, protein regulator of cytokinesis 1.

and development of NSCLC, as evinced by the cell models, animal models, and clinical samples.

PRC1 accelerated proliferation of NSCLC cells through FAK signaling pathway

FAK is a cytoplasmic non-receptor protein tyrosine kinase and cytoskeleton protein, involved in *p53*, *PI3K*, and other cell signaling pathways by phosphorylation (19). FAK phosphorylation affects cell proliferation, migration, and invasion (20), and its roles in tumorigenesis of some solid tumors has been confirmed by previous research (21). In this study, we found inhibiting FAK signaling pathway could inhibit the promoting effect of *PRC1* on the proliferation of NSCLC cells, suggesting that *PRC1* may affect the proliferation of NSCLC cells by regulating FAK signaling pathway. We also verified the positive relationship between *PRC1* expression in NSCLC cells and

the phosphorylation level of the main phosphorylation sites in different functional regions of FAK (FAK pY397, FAK pY576/577, and FAK pY925). Thus, *PRC1* might accelerate NSCLC cell proliferation by promoting the phosphorylation level of multiple phosphorylation sites in FAK signaling pathway.

PRC1 promotes proliferation through FAK/paxillin signaling pathway

Our study showed that *PRC1* regulated the phosphorylation level of both FAK and paxillin pY118 by affecting the phosphorylation level of paxillin, which is in line with two previous studies (22,23). FAK/paxillin signaling pathway is closely related to the proliferation, adhesion, invasion, and metastasis of a variety of tumor cells, and therefore participates in the tumorigenesis, development, and metastasis of cancer (24). Clearly, *PRC1* can promote

Table 2 The characteristics of 150 enrolled patients

Characteristics	Number	Number of PRC1 positive expression	MOD (mean ± SD)	P
Sex				0.221
Male	91	78	12.56±4.43	
Female	59	52	10.69±3.77	
Age (years old)				0.137
≤60	87	74	10.73±3.65	
>60	63	56	12.78±5.94	
Lymphatic metastasis				<0.001
+	56	56	18.05±2.03	
-	94	74	9.53±3.72	
TNM stage				<0.001
I	52	35	8.89±1.42	
II	42	39	10.33±1.56	
III	56	56	18.05±2.03	
IV	0	0	Non-available	
Subtype of lung cancer				<0.001
Squamous cell carcinoma	38	33	9.11±2.71	
Adenocarcinoma	110	97	14.29±4.59	
Large cell lung cancer	2	0	Non-available	

MOD, mean optical density.

the proliferation of NSCLC cells by regulating the phosphorylation level of the molecules in FAK-paxillin pathway.

Relationship with cell cycle: F-actin, Cip1/p21, Kip1/p27, and pRb family

Our trial indicated that *PRC1* affected the cell cycle of tumor cells by regulating F-actin, thus promoting cell proliferation and migration. It has been reported that F-actin is a spiral fibrous polymer composed of globular actin subunits (25). F-actin plays an important role in cell adhesion, migration, apoptosis, and promotion of the invasive growth of cells (26). Current investigation implies that F-actin can regulate cytoskeleton components through integrin and FAK signal transduction pathways (27).

The cell cycle is completed through the interaction between cyclin and cyclin dependent kinase (CDK) (28). *Cip1/p21* and *Kip1/p27* are the negative regulators of the cell cycle and members of the *cyclin-dependent kinase*

inhibitor (CDKI) family, and are able to inhibit the kinase activity of a variety of cyclin and almost all cyclin-CDK complexes, therefore playing an anti-tumor role (29). This study showed that *Cip1/p21* and *Kip1/p27* expressions were significantly inhibited in NSCLC cells with a high expression of PRC1, consistent with the findings of two previous studies that show low expressions of *Kip1/p27* being associated with poor prognoses (30,31). Therefore, *Kip1/p27* was a tumor suppressor gene and could be used as an independent prognostic indicator for malignant tumors.

Cip 1/p21 is the most widely known cell cycle inhibitor protein with the most extensive inhibitory kinase activity (32). *Cip 1/p21* widely inhibits the phosphorylated kinase activity of cyclin-CDK complexes in G1 and S phases (32). The negative regulation of the cell cycle is realized by two main mechanisms: (I) the binding of *Cip1/p21* with cyclin-CDK complex inhibiting the phosphorylation of pRb, and thus stagnating the cell cycle; (II) the binding of *Cip 1/p21* with proliferating cell nuclear antigen forming a complex to inhibit DNA replication

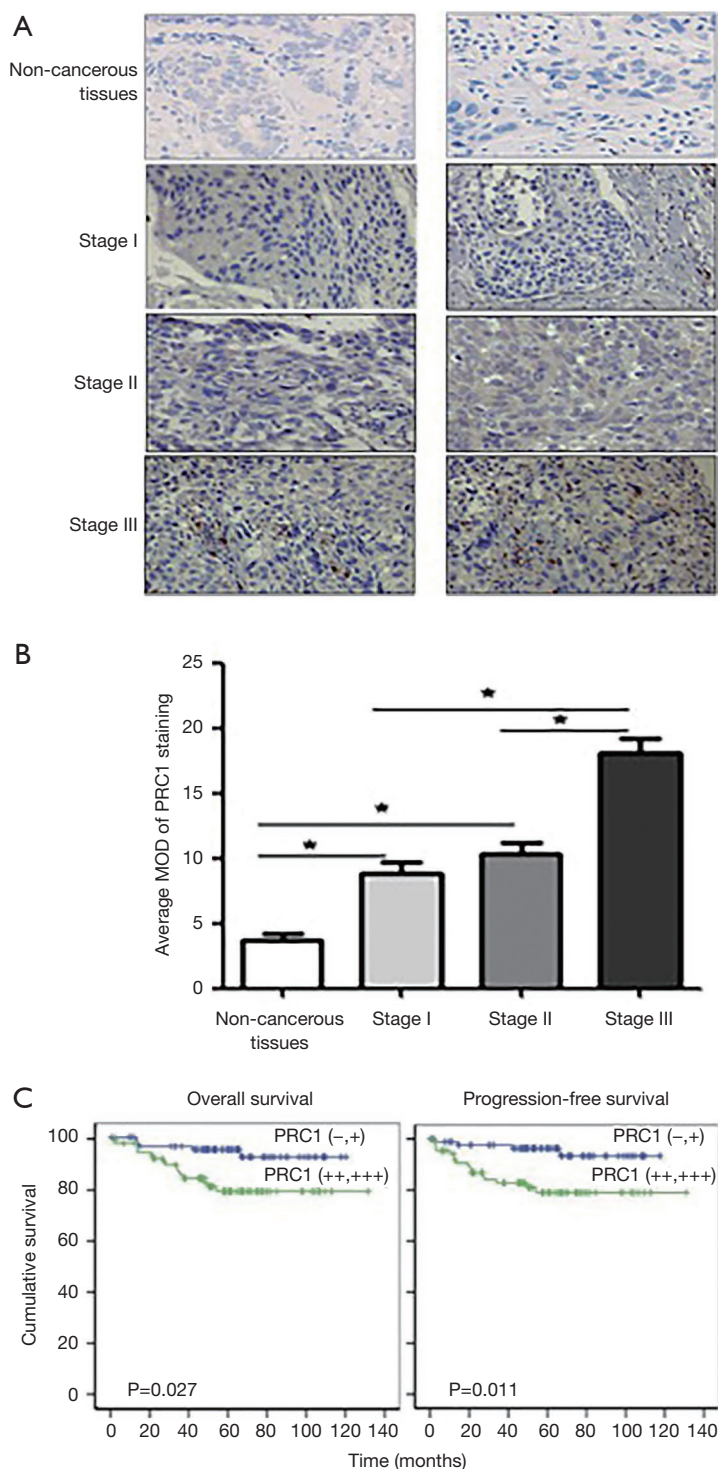


Figure 5 The relationship between *PRC1* expression and patients' characteristics. MOD refers to mean optical density. (A) The results of immunohistochemistry of patients with different TNM stage. The tissues were stained by diaminobenzidine. The color was tan when *PRC1* was expressed ($\times 200$). (B) Comparison of the MOD value of patients with different TNM stage. (C) The relationship between *PRC1* expression and the prognosis of NSCLC. *PRC1*, protein regulator of cytokinesis 1; MOD, mean optical density.

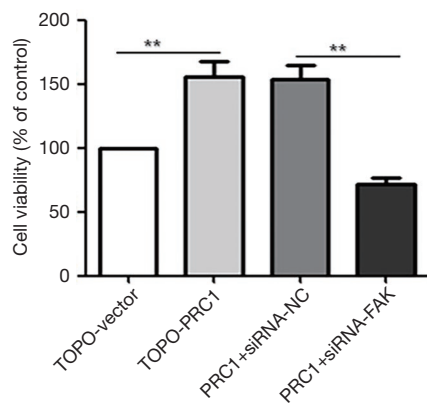


Figure 6 The cell proliferation capacity among different groups. Cells transfected with highly expressed *PRC1* plasmids, empty vector, siRNA-*PRC1*, and siRNA-negative control were divided into the TOPO-*PRC1* group, TOPO-Vector group, siRNA-*PRC1* group, and siRNA-NC group, respectively. *PRC1*, protein regulator of cytokinesis 1.

and stagnate the cell cycle in the G1 phase (33). A similar function is also found between Cip1/p21 and Kip1/p27, but a lower inhibitory effect on the tumor cell cycle is present in Cip1/p21 than in Kip1/p27 (34). Given this, the deletion of Cip1/p21 in tumor may be a promising prognostic indicator.

Strengths and limitations

This study verified the role of *PRC1* in the development of NSCLC based on both cell models and animal models. In addition, the impact of *PRC1* on the prognosis of patients strongly indicated us that the therapy targeted to *PRC1* is a promising regimen to improve the survival of NSCLC patients. Nevertheless, this work inevitably had some limitations. First, the limited sample size restricted us to exclude the possibility that some lung cancer cells mainly follow other alternative signaling pathways related

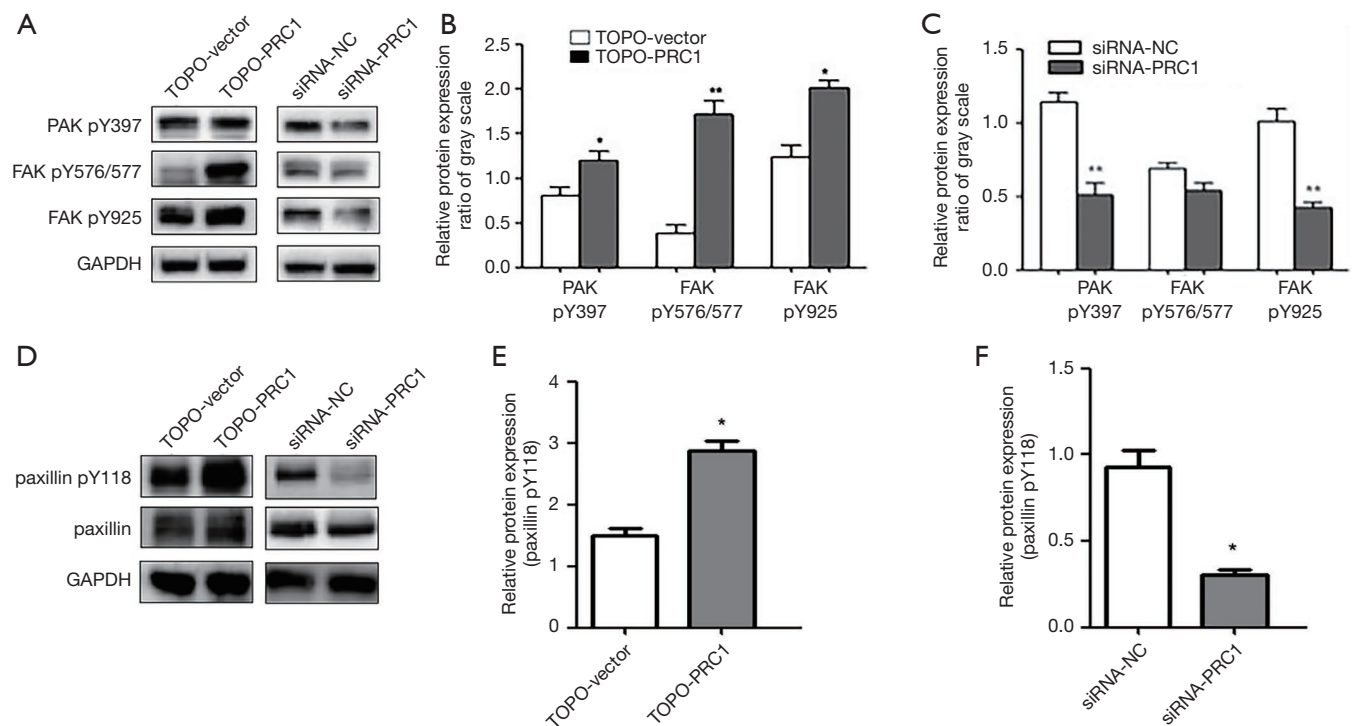


Figure 7 The phosphorylation level of major phosphorylation sites of NSCLC cells and paxillin in different groups. Cells transfected with highly expressed *PRC1* plasmids, empty vector, siRNA-*PRC1*, and siRNA-negative control were divided into the TOPO-*PRC1* group, TOPO-Vector group, siRNA-*PRC1* group, and siRNA-NC group, respectively. (A) The phosphorylation levels of NSCLC cells in the 4 groups. (B) Quantitative analysis of protein grayscale in the TOPO-vector and TOPO-*PRC1* group. (C) Quantitative analysis of protein grayscale in the siRNA-NC and siRNA-*PRC1* group. (D) The expression and phosphorylation levels of paxillin in the 4 groups. (E) Quantitative analysis of paxillin in the TOPO-vector and TOPO-*PRC1* group. (F) Quantitative analysis of paxillin in the siRNA-NC and siRNA-*PRC1* group. *PRC1*, protein regulator of cytokinesis 1.

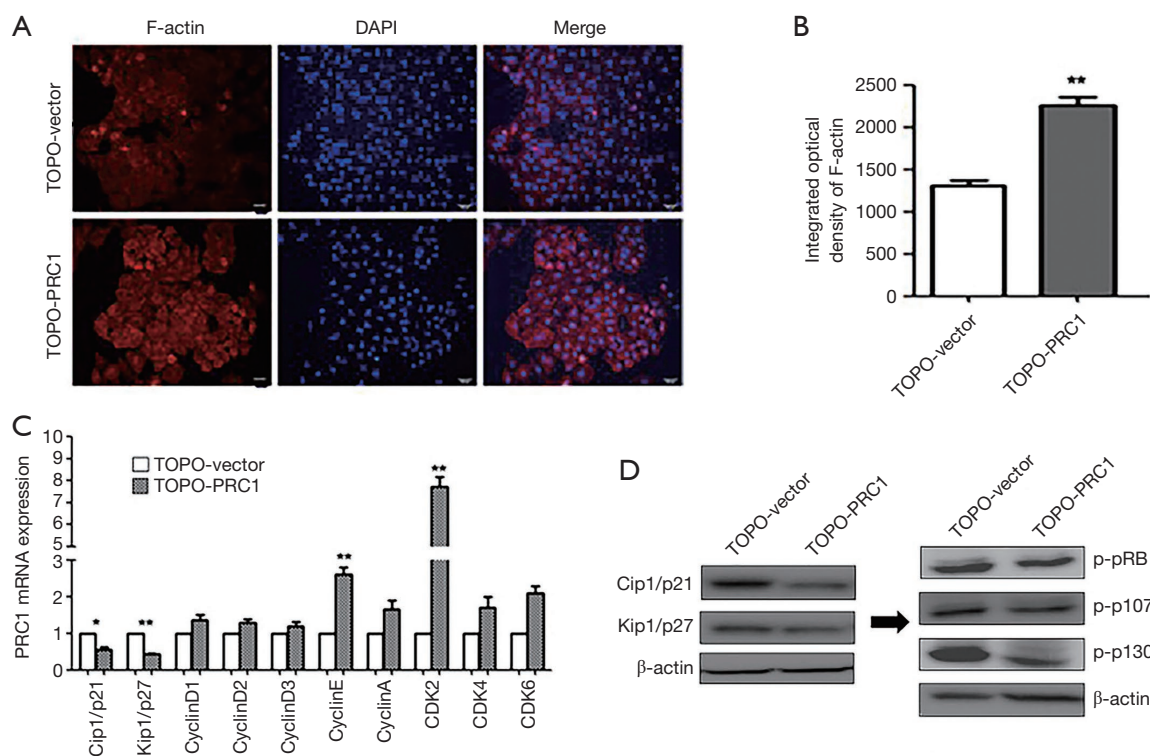


Figure 8 The expression and phosphorylation of molecules related to the NSCLC cell cycle in different groups. Cells transfected with highly expressed *PRC1* plasmids, empty vector, siRNA-*PRC1*, and siRNA-negative control were divided into the TOPO-*PRC1* group, TOPO-Vector group, siRNA-*PRC1* group, and siRNA-NC group, respectively. IOD refers to immunofluorescence intensity. (A) The expression of F-actin in different groups by immunofluorescence ($\times 200$). (B) The IOD of NSCLC cells in the 4 groups. (C) The mRNA expression of molecules related to the NSCLC cell cycle in the different groups by q-PCR. (D) The expression of Cip1/p21 and Kip1/p27, and the phosphorylation of p107, p130, and pRb. NSCLC, non-small cell lung cancer; *PRC1*, protein regulator of cytokinesis 1.

to *PRC1*. Second, the relationships between FAK-paxillin and cell proliferation, as well as p21/p27 or pRb and cell cycle, were demonstrated by analyzing some published researches but not in this experiment. Third, this study did not investigate the effect of epigenetic modifications related to *PRC1*. These limitations will be further solved in our future work.

Conclusions

PRC1 was significantly upregulated in tumor tissue and promoted tumor cell proliferation, migration, and cell cycle progression in NSCLC. The effects of *PRC1* were achieved by regulating the phosphorylation level of p21/p27-pRB family molecules and FAK-paxillin signaling pathway molecules, thus promoting NSCLC cell proliferation. This study indicates that *PRC1* is a key therapeutic target

for NSCLC patients, and this discovery can aid in the development of further exploration of the molecular mechanism of *PRC1* in NSCLC.

Acknowledgments

Funding: This work was supported by the Nature Science Foundation of Ningbo, China (2016A610167) and the Medical Health Science and Technology Project of Zhejiang Provincial Health Commission, China (2017KY580) (to Z Liang).

Footnotes

Conflicts of Interest: All authors have completed the ICMJE uniform disclosure form (available at <http://dx.doi.org/10.21037/tcr.2019.09.19>). The authors have no conflicts

of interest to declare.

Ethical Statement: The authors are accountable for all aspects of the work in ensuring that questions related to the accuracy or integrity of any part of the work are appropriately investigated and resolved. This study was conducted in accordance with the Declaration of Helsinki (as revised in 2013). This study was approved by the Ethics Committee of Ningbo First Hospital, and informed consent was signed by all participants.

Open Access Statement: This is an Open Access article distributed in accordance with the Creative Commons Attribution-NonCommercial-NoDerivs 4.0 International License (CC BY-NC-ND 4.0), which permits the non-commercial replication and distribution of the article with the strict proviso that no changes or edits are made and the original work is properly cited (including links to both the formal publication through the relevant DOI and the license). See: <https://creativecommons.org/licenses/by-nc-nd/4.0/>.

References

1. Siegel RL, Miller KD, Jemal A. Cancer statistics, 2018. *CA Cancer J Clin* 2018;68:7-30.
2. Allemani C, Weir HK, Carreira H, et al. Global surveillance of cancer survival 1995-2009: analysis of individual data for 25,676,887 patients from 279 population-based registries in 67 countries (CONCORD-2). *Lancet* 2015;385:977-1010.
3. Torre LA, Bray F, Siegel RL, et al. Global cancer statistics, 2012. *CA Cancer J Clin* 2015;65:87-108.
4. Gao D, Vahdat LT, Wong S, et al. Microenvironmental regulation of epithelial-mesenchymal transitions in cancer. *Cancer Res* 2012;72:4883-9.
5. Wang DC, Wang W, Zhu B, et al. Lung Cancer Heterogeneity and New Strategies for Drug Therapy. *Annu Rev Pharmacol Toxicol* 2018;58:531-46.
6. Liu J, Lee W, Jiang Z, et al. Genome and transcriptome sequencing of lung cancers reveal diverse mutational and splicing events. *Genome Res* 2012;22:2315-27.
7. Warth A, Penzel R, Lindenmaier H, et al. EGFR, KRAS, BRAF and ALK gene alterations in lung adenocarcinomas: patient outcome, interplay with morphology and immunophenotype. *Eur Respir J* 2014;43:872-83.
8. Lopez-Chavez A, Thomas A, Rajan A, et al. Molecular profiling and targeted therapy for advanced thoracic malignancies: a biomarker-derived, multiarm, multihistology phase II basket trial. *J Clin Oncol* 2015;33:1000-7.
9. Tang H, Xiao G, Behrens C, et al. A 12-gene set predicts survival benefits from adjuvant chemotherapy in non-small cell lung cancer patients. *Clin Cancer Res* 2013;19:1577-86.
10. Shrestha S, Wilmeth LJ, Eyer J, et al. PRC1 controls spindle polarization and recruitment of cytokinetic factors during monopolar cytokinesis. *Mol Biol Cell* 2012;23:1196-207.
11. Kurasawa Y, Earnshaw WC, Mochizuki Y, et al. Essential roles of KIF4 and its binding partner PRC1 in organized central spindle midzone formation. *EMBO J* 2004;23:3237-48.
12. Mollinari C, Kleman JP, Saoudi Y, et al. Ablation of PRC1 by small interfering RNA demonstrates that cytokinetic abscission requires a central spindle bundle in mammalian cells, whereas completion of furrowing does not. *Mol Biol Cell* 2005;16:1043-55.
13. Ganguly A, Yang H, Sharma R, et al. The role of microtubules and their dynamics in cell migration. *J Biol Chem* 2012;287:43359-69.
14. Cirillo L, Gotta M, Meraldi P. The Elephant in the Room: The Role of Microtubules in Cancer. *Adv Exp Med Biol* 2017;1002:93-124.
15. Luo HW, Chen QB, Wan YP, et al. Protein regulator of cytokinesis 1 overexpression predicts biochemical recurrence in men with prostate cancer. *Biomed Pharmacother* 2016;78:116-20.
16. Chen J, Rajasekaran M, Xia H, et al. The microtubule-associated protein PRC1 promotes early recurrence of hepatocellular carcinoma in association with the Wnt/beta-catenin signalling pathway. *Gut* 2016;65:1522-34.
17. Zhan P, Xi GM, Liu HB, et al. Protein regulator of cytokinesis-1 expression: prognostic value in lung squamous cell carcinoma patients. *J Thorac Dis* 2017;9:2054-60.
18. Zhan P, Zhang B, Xi GM, et al. PRC1 contributes to tumorigenesis of lung adenocarcinoma in association with the Wnt/beta-catenin signaling pathway. *Mol Cancer* 2017;16:108.
19. Kleinschmidt EG, Schlaepfer DD. Focal adhesion kinase signaling in unexpected places. *Curr Opin Cell Biol* 2017;45:24-30.
20. Zhao X, Guan JL. Focal adhesion kinase and its signaling pathways in cell migration and angiogenesis. *Adv Drug Deliv Rev* 2011;63:610-5.
21. Chuanyu S, Yuqing Z, Chong X, et al. Periostin promotes

- migration and invasion of renal cell carcinoma through the integrin/focal adhesion kinase/c-Jun N-terminal kinase pathway. *Tumour Biol* 2017;39:1010428317694549.
22. Miller NL, Lawson C, Kleinschmidt EG, et al. A non-canonical role for Rgnef in promoting integrin-stimulated focal adhesion kinase activation. *J Cell Sci* 2013;126:5074-85.
 23. Sachdev S, Bu Y, Gelman IH. Paxillin-Y118 phosphorylation contributes to the control of Src-induced anchorage-independent growth by FAK and adhesion. *BMC Cancer* 2009;9:12.
 24. Chen JY, Tang YA, Huang SM, et al. A novel sialyltransferase inhibitor suppresses FAK/paxillin signaling and cancer angiogenesis and metastasis pathways. *Cancer Res* 2011;71:473-83.
 25. Maruthamuthu V, Aratyn-Schaus Y, Gardel ML. Conserved F-actin dynamics and force transmission at cell adhesions. *Curr Opin Cell Biol* 2010;22:583-8.
 26. Stricker J, Falzone T, Gardel ML. Mechanics of the F-actin cytoskeleton. *J Biomech* 2010;43:9-14.
 27. Ni Y, Wang X, Yin X, et al. Plectin protects podocytes from adriamycin-induced apoptosis and F-actin cytoskeletal disruption through the integrin alpha6beta4/FAK/p38 MAPK pathway. *J Cell Mol Med* 2018;22:5450-67.
 28. Santo L, Siu KT, Raje N. Targeting Cyclin-Dependent Kinases and Cell Cycle Progression in Human Cancers. *Semin Oncol* 2015;42:788-800.
 29. Whittaker SR, Mallinger A, Workman P, et al. Inhibitors of cyclin-dependent kinases as cancer therapeutics. *Pharmacol Ther* 2017;173:83-105.
 30. Guan X, Wang Y, Xie R, et al. p27(Kip1) as a prognostic factor in breast cancer: a systematic review and meta-analysis. *J Cell Mol Med* 2010;14:944-53.
 31. Zhuang Y, Yin HT, Yin XL, et al. High p27 expression is associated with a better prognosis in East Asian non-small cell lung cancer patients. *Clin Chim Acta* 2011;412:2228-31.
 32. Kreis NN, Louwen F, Yuan J. Less understood issues: p21(Cip1) in mitosis and its therapeutic potential. *Oncogene* 2015;34:1758-67.
 33. Yoon MK, Mitrea DM, Ou L, et al. Cell cycle regulation by the intrinsically disordered proteins p21 and p27. *Biochem Soc Trans* 2012;40:981-8.
 34. Abukhdeir AM, Park BH. P21 and p27: roles in carcinogenesis and drug resistance. *Expert Rev Mol Med* 2008;10:e19.

Cite this article as: Liang Z, Li X, Chen J, Cai H, Zhang L, Li C, Tong J, Hu W. *PRC1* promotes cell proliferation and cell cycle progression by regulating *p21/p27-pRB* family molecules and *FAK-paxillin* pathway in non-small cell lung cancer. *Transl Cancer Res* 2019;8(5):2059-2072. doi: 10.21037/tcr.2019.09.19

Supplementary

Table S1 The gene expression profile from 3 GEO datasets

GEO datasets	Platform	Samples (test/control)	Status	Submission date
GSE8894	GPL570	62 (29/33)	Recurrence/no recurrence	Nov 20, 2007
GSE11969	GPL7015	90 (58/32)	Metastasis/no metastasis	Apr 01, 2009
GSE42127	GPL6884	133 (49/84)	ACT + good prognosis/ACT + poor prognosis	Jan 30, 2013

ACT, adjuvant chemotherapy.

Table S2 The primers used in q-PCR

Gene	Forward primer	Reverse primer
<i>PRC1</i>	5'- GCTGAGATTGTGCGGTTA-3'	5'- GCCTTCAACTCTTCTTCCA-3'
<i>GAPDH</i>	5'-TGACTTCAACAGCGACACCCA-3'	5'-CACCCGTGTGCTGTAGCCAAA-3'

Table S3 Detailed information about sequence used in plasmid construction and cell transfection

Plasmid	Sense (5'-3')	Antisense (5'-3')
PRC1-Homo-1816	GGAAAGCGCUGCAAUUAGATT	UCUAAUUGCAGCGCUUUCCTT
PRC1-Homo-1749	CUGAGGUGGUAAAAGAAGCATT	UGCUUCUUUACCACCUCAGTT
PRC1-Homo-852	CUGUGCGAAAUUCUUUGUATT	UACAAAGAAUUUCGCACAGTT